

FR 860 25 04

COMMISSARIAT A L'ENERGIE ATOMIQUE

CENTRE D'ETUDES NUCLEAIRES DE SACLAY

Service de Documentation

F91191 GIF SUR YVETTE CEDEX

CEA-CONF -- 8439

L3

CEA-DPh-N-S--2344

FORMATION AND DECAY OF HOT NUCLEI

CASSAGNOU, Y.; CONJEAUD, M.; DAYRAS, R.; and others

CEA CEN Saclay, 91-Gif-sur-Yvette (France). IRF, DPh-N

Communication présentée à : Symposium on the many facets of ion fusion reaction
Argonne, IL (USA)
24-26 Mar 1986

FORMATION AND DECAY OF HOT NUCLEI

Y. Cassagnou, M. Conjeaud, R. Dayras, S. Harar, R. Legrain,

M. Mostefaï, E.C. Pollacco, C. Volant

Service de Physique Nucléaire - Basse Energie

CEN Saclay, 91191 Gif-sur-Yvette Cedex, France

and

G. Klotz-Engmann, H. Oeschler

Inst. Für Kernphysik, TH Darmstadt, Germany

The aim of the present investigation is to determine the entrance channel conditions to form nuclei as hot as possible and also to study their decay properties.

The experiment has been realised at the GANIL facility using ^{14}N , ^{40}Ar and ^{58}Ni projectiles at intermediate energies and with beam intensities ranging from 100 to 500 nA. The technique we used to determine the linear momentum imparted to the target nucleus is the angular correlation of the fission products, whereas energies deposited in nuclei were deduced from the measurement of masses and velocities of both fission fragments.

The first study concerns the ^{40}Ar induced fission on ^{232}Th target at energies ranging from 31 to 44 MeV/u¹.

The main features are presented in fig.1 ;

- i) A prominent peak is observed at relative angle $\theta_{ff} \approx 170^\circ$ corresponding to sequential fission induced by quasi-elastic collisions ($\bar{p}_\parallel \approx 0.8$ GeV/c).
- ii) A bump located at high momentum transfer ($\theta_{ff} \approx 110^\circ$ corresponding to $\bar{p}_\parallel \approx 7$ GeV/c) which can be attributed to central collisions. These events result from incomplete fusion process since their recoil velocities are lower than the one corresponding to full momentum transfer (arrows in fig.1a) Two aspects are very striking ; the disappearance of the bump at 44 MeV/u and the fixed average momentum transfer with incident energies.

The different nature of the two main processes appearing in the angular correlations, i.e. peripheral and central collisions is illustrated in fig.1b, c. For quasi-elastic sequential fission, the total mass \bar{M}_{tot} of the detected fission fragments is rather constant with incident energies as

expected from a perturbative process. In contrast \bar{M}_{tot} decreases significantly with energy for central collisions since higher temperatures are reached in the fusion-fission process.

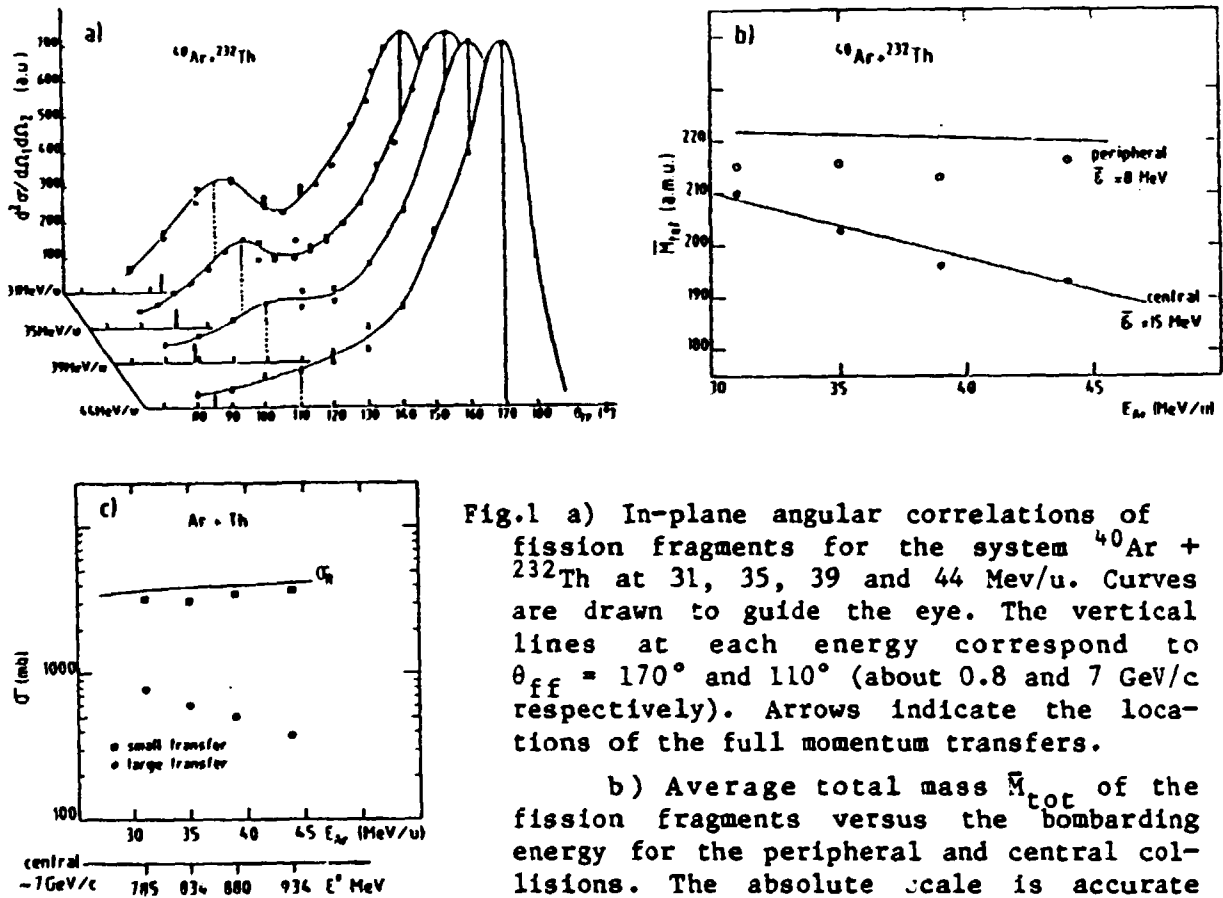


Fig.1 a) In-plane angular correlations of fission fragments for the system $^{40}\text{Ar} + ^{232}\text{Th}$ at 31, 35, 39 and 44 MeV/u. Curves are drawn to guide the eye. The vertical lines at each energy correspond to $\theta_{\text{ff}} = 170^\circ$ and 110° (about 0.8 and 7 GeV/c respectively). Arrows indicate the locations of the full momentum transfers.

b) Average total mass \bar{M}_{tot} of the fission fragments versus the bombarding energy for the peripheral and central collisions. The absolute scale is accurate within ± 5 amu, whereas relative uncertainties are smaller than the point sizes. The curves are results of calculations using

the massive transfer hypothesis with average energy $\bar{\epsilon}$ per nucleon removed by evaporation as indicated on the figure.

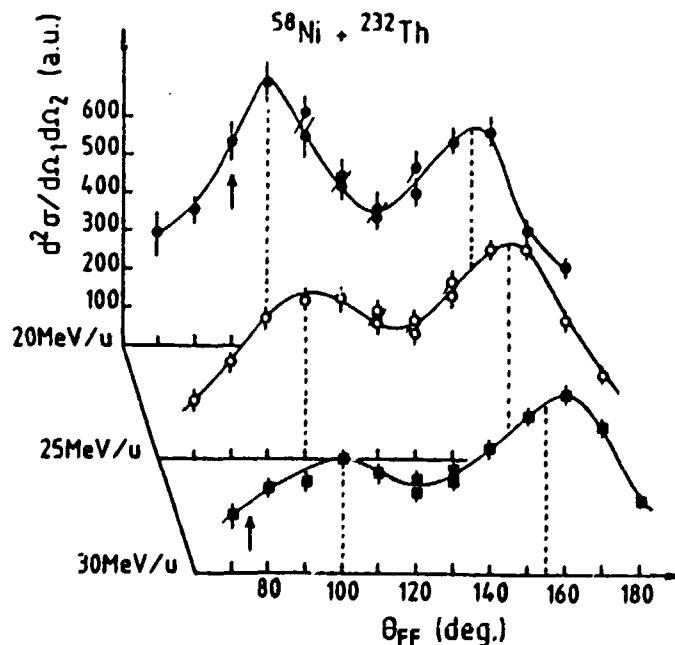
c) Estimated cross sections for peripheral (rectangles) and central (points) collisions of the Ar + Th induced fission at different incident energies. The curve is the reaction cross section calculated using optical to model parameters from ref.2.

Excitation functions, fig.1c, for both peripheral and central collisions are discussed elsewhere¹ in some details. But here again, one observes that the yield corresponding to large \bar{p}_\parallel (> 4 GeV/c) decreases with incident energies, whereas for small \bar{p}_\parallel (< 4 GeV/c) it is rather constant. Within the experimental uncertainties, the sum of these two contributions exhaust the

reaction cross section at low incident energies and leaves the room at higher energies, of few hundred millibarns for processes other than binary fission. In order to determine if the washing out of the bump at 44 MeV/u is due to the maximum excitation energy acceptable by nuclei or, to entrance channel conditions, we studied the Ni + Th system which allows the introduction of more momentum and excitation energies into the target nuclei at the same relative velocities as for the Ar + Th measurement.

Experimental results are presented in fig. 2. The main difference is that now the bump corresponding to central collisions is located at $\bar{p}_{ff} = 9.5$ GeV/c which implies in the massive transfer framework, fissioning nuclei with $A \sim 270$ at about 900 MeV excitation energy. This result suggests that the disappearance of the bump observed at 44 MeV/u Ar is not due to a limiting excitation energy in the composite like system since in both Ni and Ar induced incomplete fusion a temperature of about 5 MeV is reached ; hence entrance channel properties play an essential role in fixing the central collision yields.

Fig.2 - In-plane angular correlation of fission fragments for the $^{58}\text{Ni} + ^{232}\text{Th}$ systems at different incident energies. The vertical lines correspond to $\theta_{ff} = 155^\circ$ and 100° (about 1 and 9.5 GeV/c respectively). Arrows indicate the location of the full momentum transfers.



At this stage, several remarks can be pointed out ;

- 1) The disappearance of the bump at 44 MeV/u Ar does not mean that fission events corresponding to high momentum transfers ($\bar{p} > 7$ GeV/c) cannot be produced by such entrance channels. In fact, when studying the Ar induced

fission on ^{165}Ho for which peripheral collisions are strongly suppressed because of the fission barrier height, one observes, that high momentum transfers are imparted to target (fig.3). Several reaction mechanisms are probably involved in central collisions ranging between both nucleus-nucleus and nucleon-nucleon interactions.

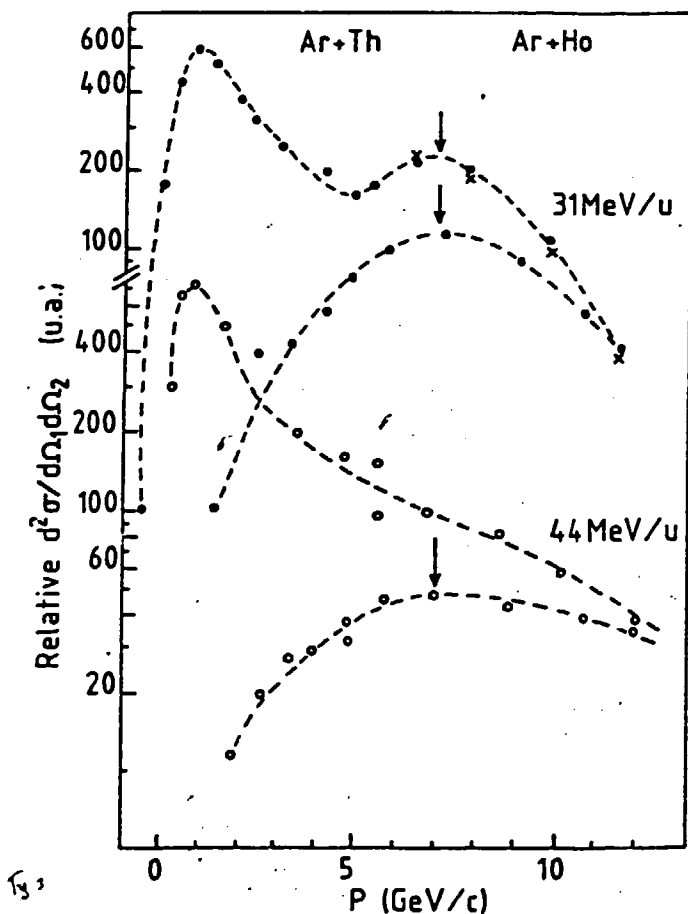


Fig.3 - In-plane angular correlations for the fission fragment for $^{40}\text{Ar} + ^{232}\text{Th}$ and $^{40}\text{Ar} + ^{165}\text{Ho}$ systems at 31 and 44 MeV/u.

The present data could indicate that the one body dissipation is vanishing for such entrance channel while two body dissipation still contributes to the population of hot nuclei.

ii) The relative velocity of 44 MeV/u Ar projectiles is not sufficient to explain such transition since higher velocity projectiles such as ^{14}N at 60 MeV/u on Th can induce a shoulder in the central collision region (fig.4). It is probably both the velocity and size of the projectiles which determine the nature of mechanisms involved in these central collisions. Further as expected, one observes that 250 MeV/u ^{14}N induced fission yield essentially peripheral collisions with more violent collisions decaying

mainly by multifragmentation processes.

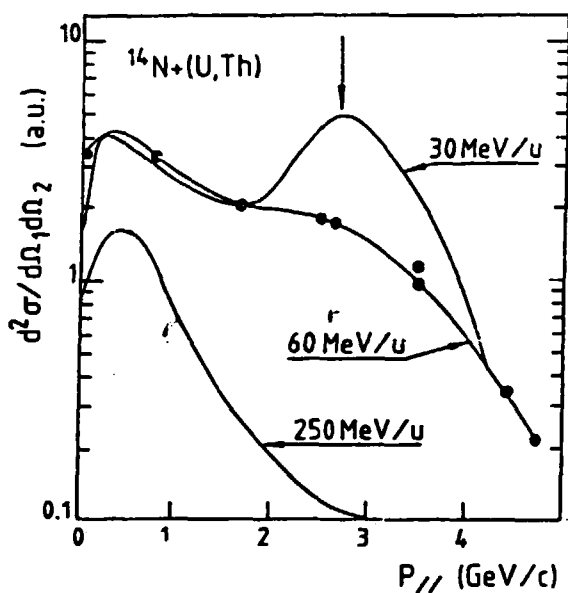


Fig.4 - In-plane angular correlation of the $^{14}\text{N} + \text{U}$ at 30 MeV/u ref.4, and $^{14}\text{N} + ^{232}\text{Th}$ at 60 and 250 MeV/u measured at GANIL and Saturne respectively.

iii) Average momentum transfers are saturated at 2.6 GeV/c, 7 GeV/c and 9.5 GeV/c for ^{14}N , ^{40}Ar and ^{58}Ni respectively. These values are not significantly dependent of the target nuclei for masses > 165 amu. Thus one observes a remarkable scaling of momentum imparted to target nuclei with the projectile masses since $\bar{P}_{\parallel} = (180 \pm 20)\text{MeV}/c$. This result is very important since it indicates that the whole projectile interacts with the target nuclei and that each escaping nucleon carries away more than 180 MeV/c in average. Another way to present this result is illustrated in fig.5, by plotting the ratio of the momentum transfer on incident momentum versus the relative velocity of the colliding ions. The solid line is obtained assuming that each projectile nucleon can transferred a fixed value of 180 MeV/c to the target nuclei at all incident energies above 15 MeV/u. We performed recently some calculations using the exciton model³ which are presented in table 1. The total momentum transfers fit quite well the experimental results and excitation energies are compatible with those deduced from masses and velocities of the fission fragments¹. When assuming a massive transfer picture to fit the experimental \bar{p}_{\parallel} values, one deduces quite similar excitation energies, Table 1, as obtained with the preequilibrium model, while the basic assumptions are very different.

TABLE I
 $^{58}\text{Ni} + ^{232}\text{Th}$

E_i (MeV/u)	Massive m_{out} (amu)	transfer ^{a)} E^* (MeV)	Precompound model \bar{P}_1 (GeV/c)	m_{pre} (amu)	E^* (MeV)
20	9	813	9.56	9.5	716
25	14.5	920	10.	13.3	830
30	18	1000	10.3	17.2	927

$^{40}\text{Ar} + ^{232}\text{Th}$

31	11	785	7.36	11.2	734
35	13	834	7.52	13	793
39	14.5	880	7.62	14.6	851
44	16	934	7.76	16.8	914

a) For the massive transfer, \bar{P}_1 is deduced from the angular correlation while it is predicted in the precompound model. E^* are deduced without taking into account the Q values.

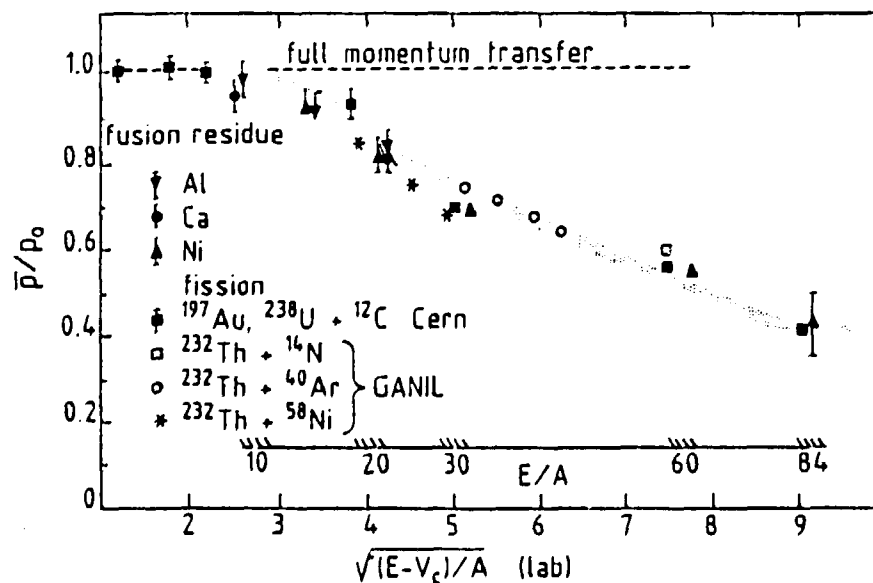


Fig.5 - Average momentum transfer for central collisions on projectile momentum versus the square root of the incident energy per nucleon above the Coulomb barrier.

This is traced to the fact that in the exciton model the escaping nucleons are concentrated at forward angles and carry away approximately the same total energies (kinetic plus binding energies) as the spectator nucleon in the massive transfer picture. However, the determination of the origin of the momentum transfer saturation needs further studies both experimental and theoretical.

Another fascinating aspect of the present experiment concerns the recoil properties of fission fragments. Two dimensional plot of the coincident fission fragment masses are presented in fig.6 for both low (~ 1 GeV/c) and high (~ 9.5 GeV/c) momentum transfers. For these two conditions, the fission region is well defined, but for central collisions the mass asymmetry becomes rather large. The relative velocities (\bar{V}_{ff}) versus the total detected mass presented in the right part of fig.6 are well fitted by the Viola systematics showing that the observed fission process is an usual one for peripheral collisions. In contrast for violent collisions, the velocity distribution is shifted towards higher values showing a tail up to 2 cm/ns which represents quite abnormal total kinetic energies for fission processes. This effect might be due to a compact configuration on the saddle point and partly to angular momentum effect.

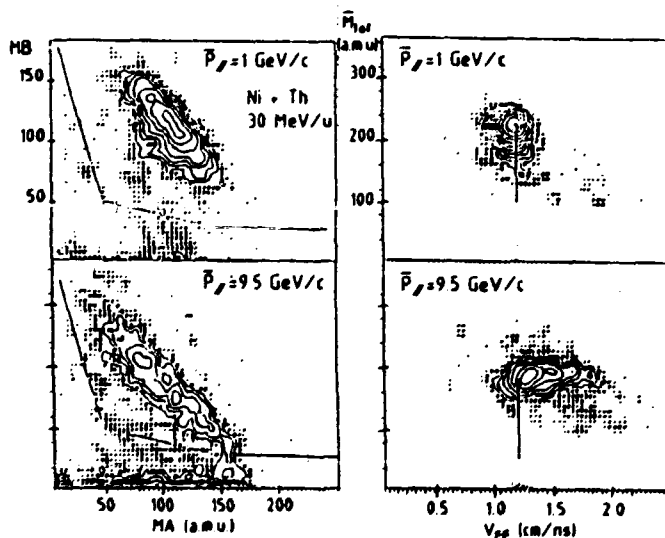


Fig.6 - Two-dimensional plot of fission fragment detected in coincidences at low and high momentum transfers (left part) and of the total detected mass of the fission fragment versus its relative velocities (right part). Arrows indicate the relative velocity from Viola systematics.

In summary, important amount of momentum transfers and excitation energies have been imparted to composite-like-nuclei with $A \approx 270$. A scaling for momentum transfer with the projectile mass is evidenced up to the Ni ions for central collisions. Velocity and size of projectiles play an important role as well as excitation energies deposited in fissioning nuclei, in fixing the central collision cross sections. Finally, high relative velocities of fission fragments have been measured and open an interesting problem on the fission properties of nuclei at high excitation energies and angular momenta.

REFERENCES

- 1) E.C. Pollacco et al., Phys. Lett. 146B (1986) 29 ;
M. Conjeaud et al., Phys. Lett. 159B (1985) 244.
- 2) N. Alamanos et al., Phys. Lett. 137B (1984) 37.
- 3) M. Blann, Phys. Rev. C31 (1985) 1245.
- 4) M. Fatyaga et al., Phys. Rev. Lett. 55 (1985) 1376.